Physics

Electricity & Magnetism fields

Okayama University   *Year* 1999

Investigation of evolution strategy and optimization of induction heating model

Makoto Horii[*]   Norio Takahashi[†]

Takashi Narita[‡]

[*]Okayama University

[†]Okayama University

[‡]Shinko Electric Corporation Limited

Investigation of Evolution Strategy and Optimization of Induction Heating Model

Makoto Horii, Norio Takahashi, *Fellow, IEEE*, and Takashi Narita

Abstract—An optimal design method using the finite element method and the evolution strategy (ES) is investigated. The evolution strategy is applied to the optimization of induction heating model. The position of auxiliary coil, frequency and ampere-turns are optimized so that the distribution of eddy current density on the surface of steel becomes uniform. It is shown that the selection of the appropriate parameter is important in the practical application of ES.

Index Terms—Evolution strategy, induction heating model, optimization, standard deviation.

I. INTRODUCTION

VARIOUS optimization methods, such as a direct search method, an evolution strategy (ES) [1]–[3], a simulated annealing method (SAM) [4], have been applied to the optimal design of magnetic devices. ES and SAM are used to find the global minimum of objective function. But, the effects of various parameters of ES, such as the initial value of standard deviation, on the convergence characteristic and the CPU time were not investigated using actual magnetic devices. Therefore, the criterion for selecting optimal values of these parameters was not clear.

In this paper, factors affecting the convergence characteristic and CPU time of ES are investigated. ES is applied to the optimal design of induction heating device [5] which is proposed by the "Investigation Committee on Highly Advanced Optimization Technique for Electromagnetic Problems," IEE of Japan. It is shown that the selection of the appropriate parameter is important in the practical application of ES.

II. INITIAL VALUE OF STANDARD DEVIATION OF (1+1)-ES

(1+1)-ES is the method that generates one child vector from one parent vector comparing two objective functions of each vector. The vector with a good objective function is treated as a parent vector of next generation.

The child vector is defined by the following equation (mutation):

$$x_c^{(k)} = x_p^{(k)} + N_n(0, \sigma^2(j)) \tag{1}$$

where $\boldsymbol{x}_p^{(k)}$ is a parent vector of the kth generation, and $\boldsymbol{x}_c^{(k)}$ is a child vector. $N_n(0, \sigma^2(j))$ is a normal random vector ($\sigma(j)$:
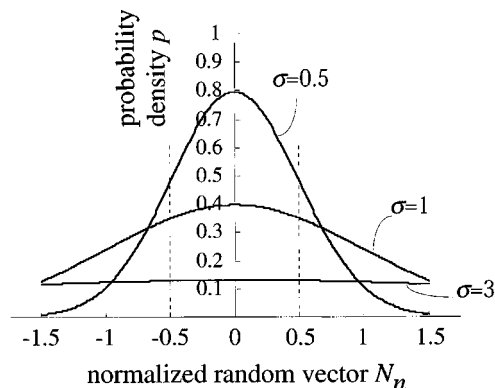
Fig. 1. Normalized distribution of probability density.

standard deviation, j: number of times that Rechenberg's 1/5 success law is carried out, n: number of design variables).

The parent vector of next generation is determined as follows by comparing the objective function W_p of the parent vector and W_c of the child vector (selection):

$$\boldsymbol{x}_p^{(k+1)} = \begin{cases} \boldsymbol{x}_c^{(k)} & (W_c \leq W_p) \\ \boldsymbol{x}_p^{(k)} & (W_c > W_p) \end{cases} \tag{2}$$

Eq. (2) denotes that if the objective function W_c of the child vector $\boldsymbol{x}_c^{(k)}$ is smaller than W_p of the parent vector $\boldsymbol{x}_p^{(k)}$, the child vector $\boldsymbol{x}_c^{(k)}$ is adopted as the parent vector $x_p^{(k+1)}$ at the $(k+1)$th generation. If W_c of the child vector $\boldsymbol{x}_c^{(k)}$ is larger than W_p of the parent vector $\boldsymbol{x}_p^{(k)}$, the child vector $\boldsymbol{x}_c^{(k)}$ is not chosen at the parent vector $x_p^{(k+1)}$ at the $(k+1)$th generation.

But, the evolution is not good if optimized using only the mutation and selection operations. Then, Rechenberg's 1/5 success law, which changes the standard deviation at every several iterations, is used. The standard deviation $\sigma(j+1)$ is decided by the following equation, according to the value of the probability P_s that the objective function gets smaller in, for example, 20 (= 10× (number of design variables)) generations:

$$\sigma(j+1) = \begin{cases} \sigma(j) \cdot c_d & (P_s < \frac{1}{5}) \\ \sigma(j) & (P_s = \frac{1}{5}) \\ \sigma(j)/c_d & (P_s > \frac{1}{5}) \end{cases} \tag{3}$$

where c_d is a constant less than unity ($0.817 \leq c_d < 1.0$).

Fig. 1 shows the normalized distribution of probability density at $\sigma = 0.5$, 1.0 and 3.0. If an initial value of a design variable is chosen as a middle value of its constraint (range of the amplitude of design variables), the normalized constraint N_n is within ± 0.5 from the initial value. If the initial value σ_0 is equal to 0.5, the probability of searching a solution is higher (probability density p is nearly equal to 0.8) near the parent vector,
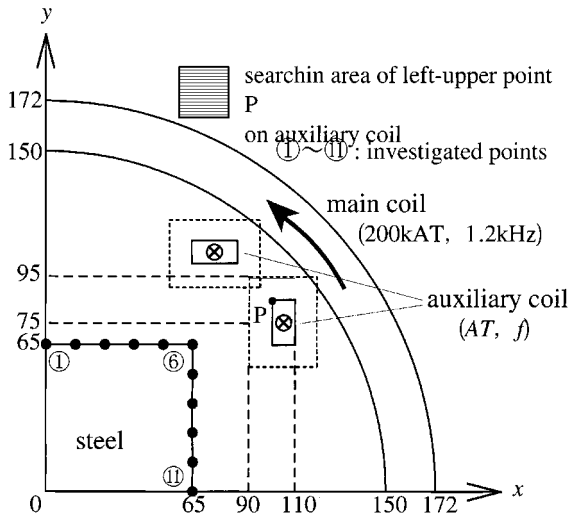
Fig. 2.   Induction heating model.

TABLE I
INITIAL VALUE AND DESIGN VARIABLE CONSTRAINTS

design variable	CONSTRAINT	initial value	
		case 1	case 2
x (mm)	$90 \le x \le 110$	100	109.9
y (mm)	$75 \le y \le 110$	85	75.1
AT (kAT)	$3 \le AT \le 9$	6	8.99
f (kHz)	$1.2 \le f \le 3.6$	2.4	1.21

TABLE II
OPTIMIZATION RESULTS (CASE 1)

σ_0	initial shape	0.01	0.05	0.1	0.5	1.0	3.0
x (mm)	100	100.2	99.3	101.8	99.1	98.0	97.5
y (mm)	85	89.7	94.4	95.0	94.5	92.2	93.9
AT (mm)	6	5.91	5.80	6.06	5.78	5.60	5.59
f (kHz)	2.4	3.46	3.59	3.60	3.58	3.59	3.59
W (10^6 A/m^2)	4.59	1.08	1.05	1.06	1.05	1.04	1.04
number of iterations	—	424	487	362	633	587	623
CPU time (s)	—	1988	2286	1742	2913	2704	2842

computer used: HP735(45MFLOPS)

TABLE III
OPTIMIZATION RESULTS (CASE 2)

σ_0	initial shape	0.01	0.05	0.1	0.5	1.0	3.0
x (mm)	109.9	109.7	108.7	96.5	103.4	97.1	98.4
y (mm)	75.1	80.7	88.4	87.4	89.7	92.4	92.7
AT (mm)	8.99	7.99	7.39	5.33	6.14	5.49	5.71
f (kHz)	1.21	2.94	3.15	3.60	3.60	3.60	3.54
W (10^6 A/m^2)	8.23	1.27	1.17	1.05	1.08	1.04	1.05
number of iterations	—	490	546	561	583	636	717
CPU time (s)	—	2234	2552	2614	2676	2859	3252

and is lower (p is nearly equal to 0.5) at the boundary of the constraint (normalized coordinate $N_n = \pm 0.5$). In the case of $\sigma_0 = 3.0$, p is almost uniform within the constraint. Therefore, the solution can be searched in the whole range of constraint, when $\sigma_0 = 3.0$.
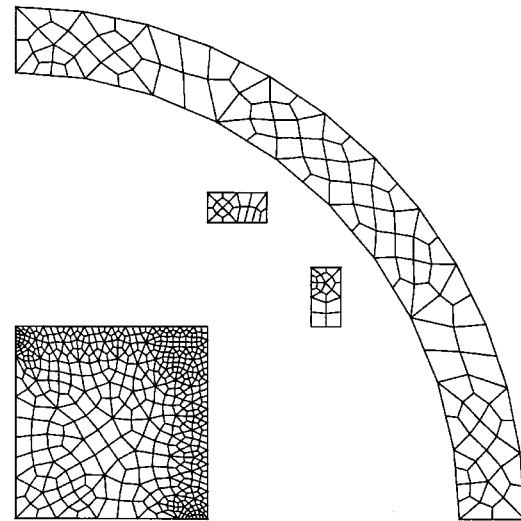
(a)
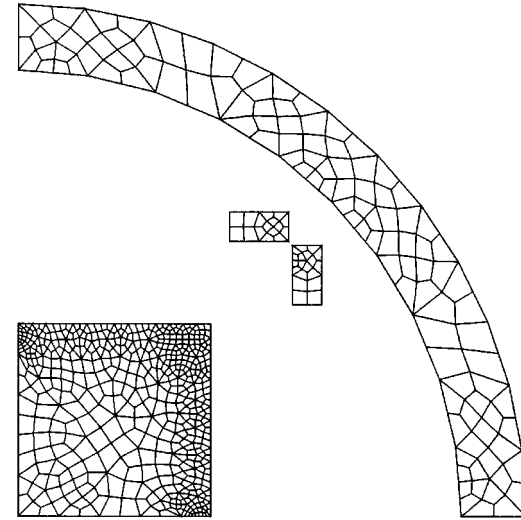
(b)

Fig. 3.   Meshes (case 1). (a) Inital shape; (b) optimal shape.

III. INDUCTION HEATING MODEL

Fig. 2 shows the induction heating model [5]. The current of the main coil flows in the x–y plane, and its ampere-turns are 200 kAT (1.2 kHz). The current of the auxiliary coil flows in the z-direction. The steel is heated by the Joule loss due to eddy current. The relative permeability of steel is assumed as unity. x- and y-coordinates of the left-upper point P of the auxiliary coil, the maximum ampere-turns AT and the frequency f of the auxiliary coil are optimized so that the distribution of eddy current density at eleven points on the surface of steel shown in Fig. 2 becomes uniform. The objective function is defined as follows:

$$W = \max\{J_{ei}\} - \min\{J_{ei}\} \tag{4}$$

where J_{ei} is the maximum value of eddy current density at the investigated point i. Table I shows the initial values and the constraint of each design variable. Two kinds of initial values of design variables, the middle value of constraint (case 1, $x = 100$ mm, $y = 85$ mm, $AT = 6$ kAT, $f = 2.4$ kHz) and the value near the boundary (case 2, $x = 109.9$ mm, $y = 75.1$ mm, $AT = 8.99$ kAT, $f = 1.21$ kHz) are chosen.
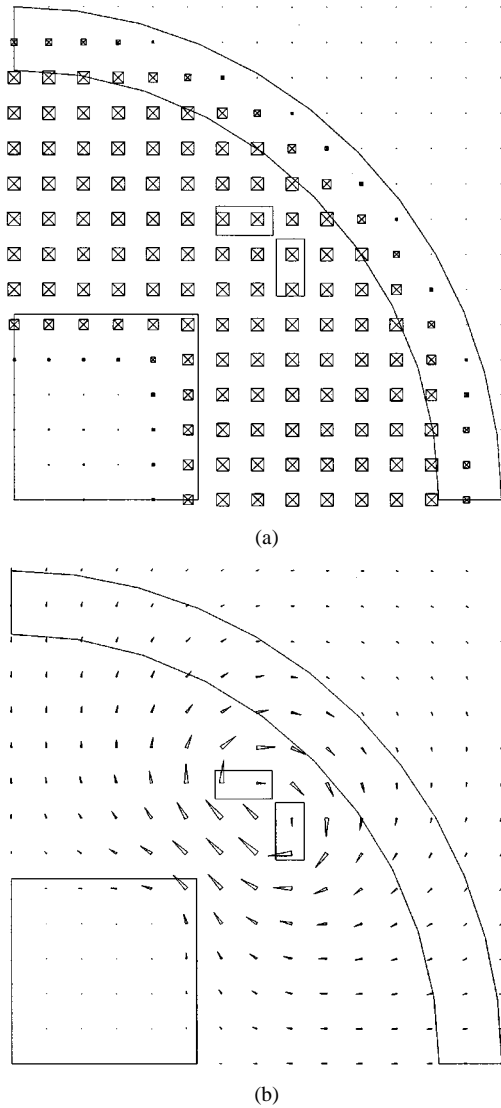
Fig. 4. Flux distribution (case 1). (a) Main coil; (b) auxiliary coil.

Fig. 5. Eddy current distributions (case 1). (a) Main coil; (b) auxiliary coil.

IV. METHOD OF ANALYSIS

The hexahedral edge elements having only one layer in the z-direction is used in the analysis. The number of elements is about 1400. The mesh is automatically produced at each iteration. As this is a linear model, first, the flux distribution is calculated when only main coil (J_{0x}^{main}, J_{0y}^{main}) is excited, and that only auxiliary coil (J_{0z}^{aux}) is excited. J_{0x}^{main} and J_{0y}^{main} denote the x- and y-components of the exciting current of main coil. J_{0z}^{aux} is the z-component of the exciting current of auxiliary coil. Second, both flux distributions are superposed. By superposing 2-D results, the CPU time can be considerably reduced compared with 3-D analysis.

Even if the frequency of the x- and y-component J_{ex}^{main}, J_{ey}^{main} of eddy current induced by the main coil is different from the z-component J_{ez}^{aux} of eddy current induced by the auxiliary coil, the maximum effective value $J_{e\max}$ of eddy current can be obtained by the following equation:

$$J_{e\max} = |\dot{\boldsymbol{J}}_e| = \sqrt{\left|\dot{j}_{ex}^{main}\right|^2 + \left|\dot{j}_{ey}^{main}\right|^2 + \left|\dot{j}_{ez}^{aux}\right|^2} \quad (5)$$

where the dot($\cdot$) means the complex number.

V. RESULTS AND DISCUSSION

Fig. 4(a) shows the flux distribution when only main coil excited and Fig. 4(b) shows that when only auxiliary coil is excited. The whole flux distribution can be obtained by superposing these flux distributions. But is should be noticed that the frequencies of these flux distributions are different with each other. Fig. 5(a) and (b) show the eddy current distributions when only main coil or auxiliary coil is excited. These figures clearly illustrate the role of each coil.

The effects of the initial value of standard deviation and initial value of design variable on the convergence are examined. σ_0 is chosen as 0.01, 0.05, 0.1, 0.5, 1.0, and 3.0. Tables II and III show the effects of initial values of standard deviation on obtained value and CPU time, and so on. When the child vector is out of the constraint of design variables, it is not counted as the number of iterations, because the finite element analysis is skipped in such a case. Tables II and III show that the smaller the initial value σ_0 of standard deviation is, the faster the convergence is. However, the solutions of smaller standard deviations are not
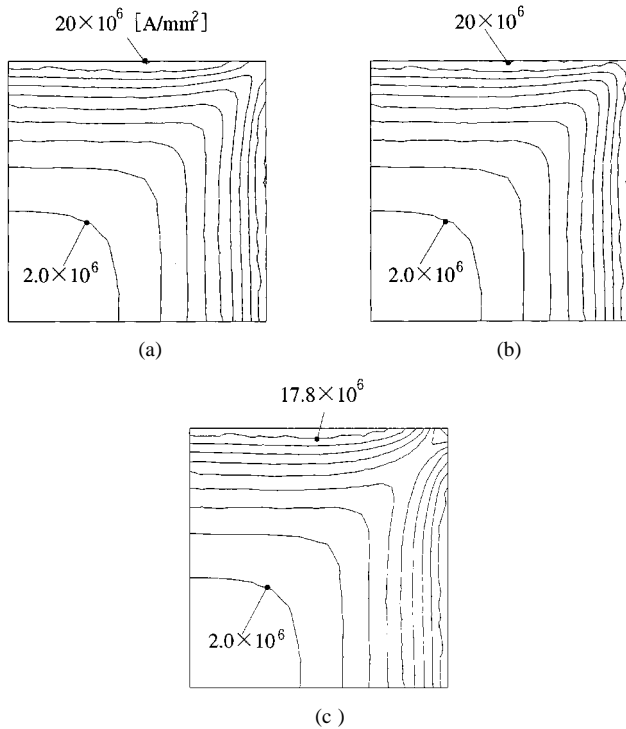
Fig. 6. Contour lines of eddy current density in steel (case 1). (a) Inital value; (b) optimal value; (c) no auxiliary coil.
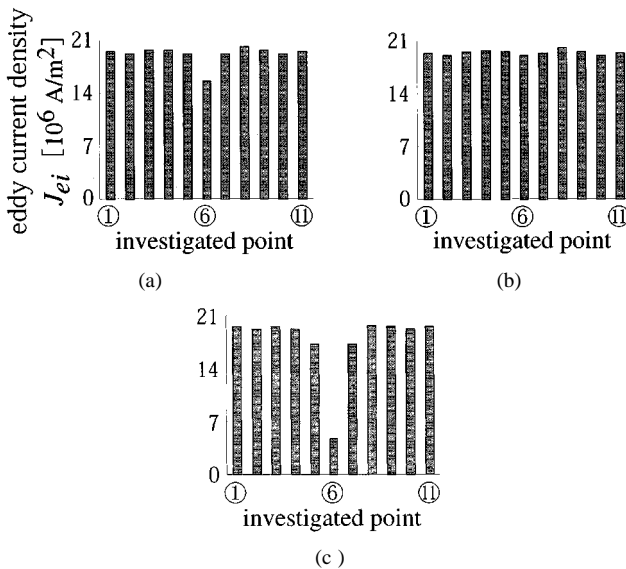

Fig. 7. Eddy current densities at investigated points (case 1). (a) Inital value; (b) optimal value; (c) without auxiliary coil.

good. The solutions at $\sigma_0 = 0.01$, 0.05, 0.1, and 0.5 fall into local minima. This suggests that the solution using ES converges to the global optimum in spite of the selection of initial values of design variables (case 2) if an initial value of the standard deviation is selected as larger than 1.0. In this paper, σ_0 is chosen as 3.0, because the solution can be searched in the whole range and the number of iterations is not so much increased compared with the case of less than $\sigma_0 = 0.5$.

Fig. 3 shows the meshes of initial and optimal shapes (case 1) at $\sigma_0 = 3.0$. Figs. 4 and 5 show flux and eddy current distri-
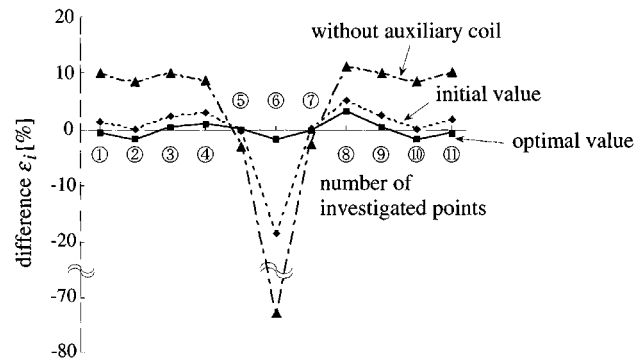

Fig. 8. Difference ε_i of eddy current density (case 1).

butions at optimal shape ($\sigma_0 = 3.0$) when only the main coil or auxiliary coil is excited. Fig. 6 shows the contour lines of eddy current density in the steel at the initial and optimal shapes (case 1) at $\sigma_0 = 3.0$ and that without auxiliary coil. Fig. 7 shows the effective eddy current densities at the investigated points. Fig. 8 shows the difference ε_i of eddy current density at the investigated point i from the average value. ε_i is defined by:

$$\varepsilon_i = \frac{J_{ei} - J_{eave}}{J_{eave}} \times 100 \ [\%] \tag{6}$$

where J_{ei} is the eddy current density at the investigated point i, and J_{eave} is the average value of J_{ei}.

VI. CONCLUSIONS

The results can be summarized as follows.

(1) It is shown that the optimal value can be obtained using the evolution strategy if the initial value of standard deviation σ_0 is selected as a suitable value, for example $\sigma_0 = 3.0$.

(2) The 3-D flux and eddy current distribution can be analyzed within acceptable CPU time by superposing two results when only main coil or auxiliary coil is excited.

(3) The position of auxiliary coil, frequency, and ampere-turns of the induction heating model can be optimized using the evolution strategy, so that the distribution of eddy current density on the surface of steel becomes uniform.

REFERENCES

[1] T. Bäck, *Evolutionary Algorithm in Theory and Practice*: Oxford University Press, 1996.
[2] K. Preis, C. Magele, and O. Biro, "FEM and evolution strategies in the optimal design of electromagnetic devices," *IEEE Trans. Magn.*, vol. 26, no. 5, pp. 2181–2183, 1990.
[3] K. Hameyer and M. Kasper, "Shape optimization of a fractional horse-power dc-motor by stochastic methods," in *Computer Aided Optimum Design Structures III, Optimization of Structural Systems and Applications, CMP*: Elsevier Applied Science, 1993, pp. 15–30.
[4] J. Simkin and C. W. Trowbridge, "Optimizing electromagnetic devices combining direct search methods with simulated annealing," *IEEE Trans. Magn.*, vol. 28, no. 6, pp. 1545–1548, 1992.
[5] H. Yamashita, H. Yamane, C. Vlatko, and K. Kaneda, "Coupled magneto-thermal analysis and optimization of induction heating equipment" (in Japanese), in *Proceedings of the Conference on Computational Engineering and Science*, vol. 3, 1998, pp. 323–326.